RESEARCH ON STRESS EVOLUTION LAW AND FAILURE CHARACTERISTICS OF TOP COAL IN FULLY MECHANIZED CAVING OF EXTRA-THICK COAL SEAMS

by

Hong-Bin LI[a,b], Dong-Yin LI[a], Hao WANG[a], Zhen-Feng LI[a], Shen WANG[a*], and Chun-Ling CHEN[a]

[a]School of Energy Science and Engineering, Henan Polytechnic University, Jiaozuo, China
[b]College of Chemistry and Chemical Engineering, Henan Polytechnic University, Jiaozuo, China

Original scientific paper
https://doi.org/10.2298/TSCI2301687L

In this study, based on the engineering background of the No. 8222 working face of the Tashan coal mine in Shanxi Province, China, true triaxial experiments were carried out on Geotechnical Consulting and Testing Systems rock mechanics testing machine using cubic coal samples, and the numerical simulation was conducted through the FLAC^{3D} software. Moreover, the stress evolution law of different layers of extra-thick coal seams and the failure mechanism of top coal in the fully mechanized caving were investigated, and the failure structure model of top coal was established. The results show that there are differences in the principal stress values at different layers of the top coal.

Key words*: extra-thick coal seams, top coal caving, stress evolution, failure structure of top coal*

Introduction

Coal plays a dominant role in China's energy structure. In 2021, China's coal output is still above 3 billion tons [1, 2], and the coal reserves of thick and extra-thick coal seams account for 45% [3-5], and their output accounts for 50% of the raw coal output [6, 7]. In the process of fully mechanized caving of thick coal seams, the mining stress field is formed around the working face due to artificial disturbance, which is also the main cause of top coal crushing [8]. Research on the evolution law of stress field and crushing mechanism of top coal during fully mechanized caving mining has been widely conducted through theoretical analysis, laboratory experiments, numerical simulation and other research methods. Kang *et al.* [9] carried out laboratory shear experiments based on Griffith's strength theory. The results revealed that the crack extension and expansion is the root cause of top coal failure, and the existing form of cracks determines the failure strength of top coal. Through theoretical analysis and numerical simulation, Huo [10] studied the stress evolution law in top coal and established a *continuous-discontinuous* 3-D numerical model. Besides, the stress evolution path was taken as the loading condition, and the crushing mechanism of top coal in the mining process of top coal mining was revealed. Alehossein *et al.* [11] defined the internal relation-

*Corresponding author, e-mail: wangshen@hpu.edu.cn

ship coefficient between yield and caving, and established the yield and caving criteria of fully mechanized top coal caving according to the original rock stress, Mohr-Coulomb/Hoek-Brown criterion and strain softening principle.

In summary, there are many studies on the stress evolution law and the crushing degree of top coal of thick coal seams. However, these studies rarely study the stress evolution law of top coal, crushing mechanism of top coal and the failure structure of top coal during the mining of extra-thick coal seams over 14 m thick. In this study, the numerical simulation was used to study the stress evolution law of top coal in different layers of extra-thick seams, and the true triaxial tests were carried out with the stress evolution law as the loading path. Besides, the crushing law of top coal at different layers under different stress paths was obtained, the distortion energy density theory was employed to reveal the crushing mechanism of top coal of extra-thick coal seams, and the failure structure model of top coal in extra-thick coal seam was developed.

Project overview

The 3#-5# coal seams were mainly exploited in the No. 8222 working face of the Tashan coal mine in Shanxi Province, China. The fully mechanized top coal caving mining was adopted, and the designed advancing length and width of the working face were 2644 m and 230 m, respectively. The coal seam was almost horizontally developed with simple structures. The average buried depth of the coal seam was 525 m, and the average thickness was 14.03 m. The mechanical mining height was 4.0 m, and the location of the working face was shown in fig. 1.

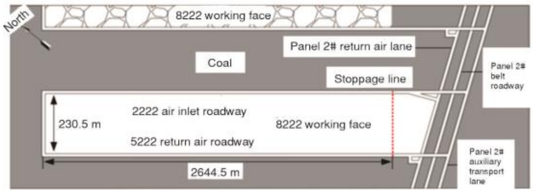

Figure 1. Layout plan of the No.8222 working face

Stress evolution law of top coal of extra thick coal seam

Establishment of numerical model

Based on the geological conditions of the No. 8222 working face in the extra-thick coal seam during the fully mechanized top coal caving, the FLAC^{3D} numerical model on the top coal caving was established. In this model, the tangential direction was taken as the *X*-axis, the trough direction as the *Y*-axis, and the vertical direction as the *Z*-axis. The total height of the model was 68 m. Five layers of overlying strata with a total height of 40 m were contained in the upper part of the coal seam, and two layers of coal seams with a total height of 14 m were contained in the floor. The lengths of the model in the *X*- and *Y*-directions were 300 m and 330 m. The model included 623040 units and 740506 calculation nodes. Figures 2 and 3 show the diagram of the numerical model.

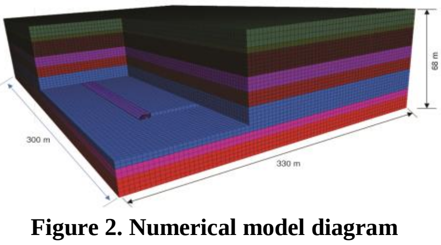

Figure 2. Numerical model diagram

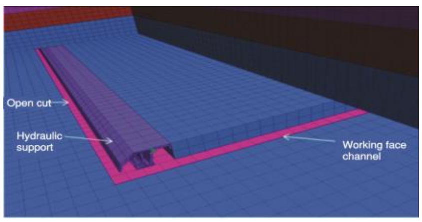

Figure 3. The hydraulic support and working face

The stress boundary of the model was set as follows. The total height of the numerical model was 68 m. The floor of the coal seam was 14 m away from the zero point in the *Z*-direction of the model, the thickness of the coal seam and the overlying strata was 54 m, and the average buried depth of the coal seam was 525 m. Therefore, the weight of the 471 m thick strata needed to be applied to the upper boundary of the model. When the average bulk density of 25 kN/m was taken, the applied stress at the upper boundary was 11.78 MPa. Besides, Normal displacement constraints were applied to the front, back, left and right of the model, and full displacement constraints were applied to the bottom of the model.

Evolution law of principal stress value and selection of characteristic points

Figure 4 shows the results of numerical simulation. Within 5 m of the hydraulic support control area of the simulated working face behind the coal wall, (*i.e.*, within the –5-0 m of the co-ordinate axis), the principal stress values of different coal seams all increase line-

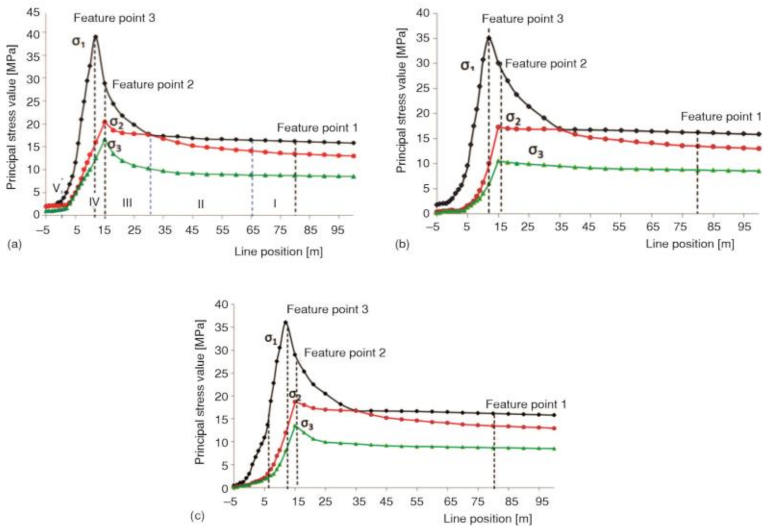

Figure 4. Evolution law of principal stress and location map of characteristic points in different layers; (a) upper coal seam, (b) central coal seam, and (c) lower coal seam

arly with small amplitude. Within the range of 0-100 m in front of the coal wall, the principal stress values of different layers increase first and then decrease along the advancing direction of the working face. The peak inflection point of different layers and principal stress values appears at 12 m in front of the coal wall. When the maximum value of σ_1 of the upper layer is 39.0 MPa, the values of σ_2 and σ_3 are 16.0 MPa and 12.5 MPa, when the maximum value of σ_1 of the lower layer is 36.0 MPa, σ_2, and σ_3 are 12.0 MPa and 8.0 MPa; when the maximum value of σ_1 of the middle layer is 35.0 MPa, σ_2 and σ_3 are 10.0 MPa and 6.0 MPa, respectively.

The stress evolution of top coal in different layers can be divided into five areas from far to near, namely, original rock stress area (Area I), slowly increasing stress area (Area II), significantly increasing stress area (Area III), decreasing stress area (Area IV), and hydraulic support roof control area (Area V). The feature points of the evolution of the principal stress field are extracted in different regions to provide the data for the subsequent true triaxial experiment on the top coal caving. The feature points of the principal stress evolution of top coal in different layers are shown in tab. 1.

Laboratory triaxial loading and unloading test of coal samples

Coal-rock true triaxial experiment system and AE monitoring system

The GCTS RTX-3000 integrated rock mechanics testing system was used in this experiment. This system was mainly composed of the hydraulic station, general digital signal regulation control unit, loading frame and pressure chamber, surrounding rock and pore water pressure booster, ultrasonic wave, and cats software, as shown in fig. 5. The experimental system can simultaneously load coal samples in three mutually perpendicular directions with equal or unequal loads. Besides, the AE activity law can be collected during the failure process of coal samples.

Table 1. Feature points of principal stress evolution of top coal in different layers

Top coal horizon	Partition	Serial number	σ_1 [MPa]	σ_2 [MPa]	σ_3 [MPa]
Lower top coal	Original rock stress zone	1	16.17	13.45	8.7
	Stress rise zone	2	29.0	18.7	13.5
		3	36.0	12.0	8.0
Middle top coal	Original rock stress zone	1	16.17	13.45	8.7
	Stress rise zone	2	26.5	17.0	10.2
		3	35.0	10.0	6.0
Top coal	Original rock stress zone	1	16.17	13.45	8.7
	Stress rise zone	2	28.8	20.4	16.55
		3	39.0	16.0	12.5

Figure 5. The RTX 3000 rock mechanics comprehensive test system

Sample preparation and loading scheme

According to the recommendations of the International Society for Rock Mechanics, the 50 × 50 × 100 mm cube samples are processed in this experiment, as shown in fig. 6. Three samples are made for each group. Since the loading and unloading steps of the three stress paths of the upper coal seam, the middle coal seam and the lower coal seam are similar. Figure 7 shows the schematic diagram of the representative true triaxial path experimental scheme for coal seams.

Figure 6. Test coal sample

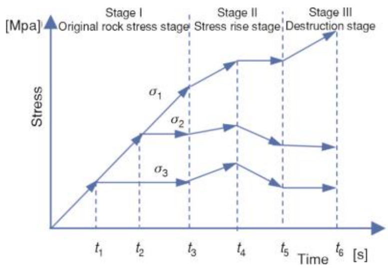

Figure 7. True triaxial loading and unloading test scheme

Deformation behavior and AE activity law of coal samples

As shown in fig. 8, in the initial loading stage, both the vertical strain and the horizontal strain increase with the increase of stress. At this stage, internal cracks are mainly closed and compacted inside the coal sample. With the continuous loading in three directions at the loading rate of 0.1 MPa/s, the horizontal area of the sample is large, and the force in the two horizontal directions is obviously larger than that in the axial direction. According to the poisson effect, tensile stress occurs in the axial direction, and the value of strain presents a negative value. The two horizontal strains show good elastic linear characteristics with the increase of stress. After tensile stress in the axial direction is increased to a certain value, the axial strain shows good elastic linear characteristics with the increase of stress. With the loading and unloading of horizontal stress and the continuous increase of vertical stress, the vertical strain of the coal sample increases constantly under the three stress paths, that is, the coal sample is in the axial compression state. The horizontal strain increases first and then decreases. It can be seen from the results that the three-dimensional stress value of the coal sample at failure during the loading and unloading experiment is similar to that of the numerical simulation, which verifies the correctness of the numerical simulation of the stress evolution of the top coal.

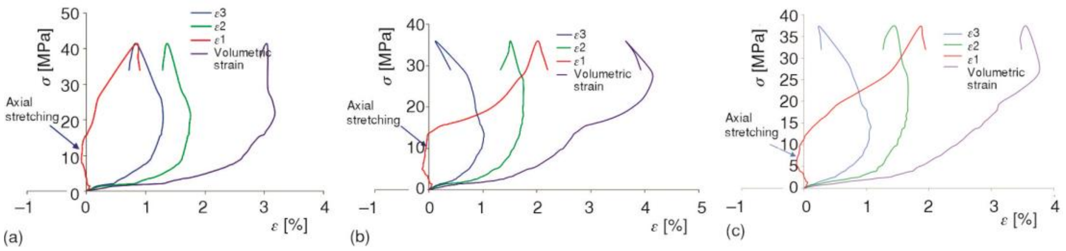

Figure 8. Deformation characteristics of the sample after loading; (a) upper coal seam, (b) central coal seam, and (c) lower coal seam

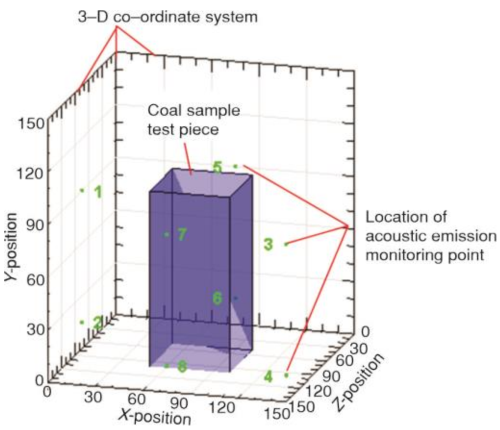

Figure 9. Location map of AE monitoring points

Based on the arrangement of acoustic emission (AE) monitoring points on the true triaxial testing machine and the corresponding coordinate setting of the monitoring points of the AE monitoring system, the AE data of coal samples in the true triaxial loading and unloading process can be located, and the damage and failure degree of coal samples in the loading and unloading process can be analyzed by the AE event location. Eight monitoring points were set in this true triaxial experiment. As shown in fig. 9, the location of AE events can be comprehensively and accurately obtained.

Figure 10 shows the localization results of AE events under different paths. It can be seen that there is the largest number of AE events under Path 2, followed by that under Path 1, and the least number of AE events in Path 3. It indicates that there is the largest damage degree inside the coal sample in Path 2, followed by that under Path 1, and the least damage degree inside the coal sample in Path 3.

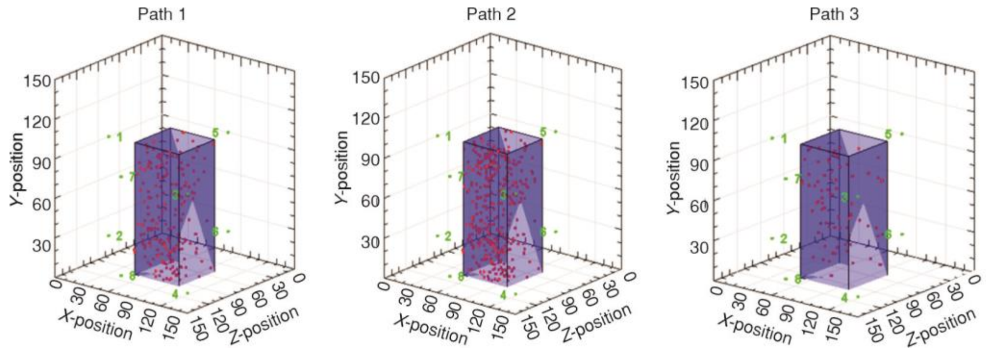

Figure 10. Location results of AE events under different paths

Breaking mechanism of top coal and failure structure model of top coal

Crushing mechanism of top coal in front of coal wall

The distortion energy density theory considers that the distortion energy density is the main factor causing yield. According to this theory, no matter what stress state, as long as the distortion energy density reaches a certain limit value related to the material properties, the material will yield. The yield criterion is given:

$$\left\{\frac{1}{2}\left[\left(\sigma_1-\sigma_2\right)^2+\left(\sigma_2-\sigma_3\right)^2+\left(\sigma_3-\sigma_1\right)^2\right]\right\}^{1/2}=\sigma_s \tag{1}$$

where σ_s is the yield stress, σ_1 – the maximum principal stress, σ_2 –the intermediate principal stress, and σ_3 – the minimum principal stress. More general case of the stress was considered in [12].

Based on the distortion energy density theory and the change law of the principal stress in different layers of extra-thick coal seams, the change law of the distortion energy density in the range of elastic deformation of coal samples can be obtained, as shown in fig. 11. It can be seen that within the range of more than 40 m in front of the coal wall, the distortion energy density, V_d. of the upper, middle and lower layers is basically the same. Within the range of 40 m to 12 m in front of the coal wall, the distortion energy density increases slowly first and then abruptly. At any measuring line, the distortion energy density is largest in the middle layer, followed by that in the lower layer, and the distortion energy density is smallest in the upper layer. It shows that under the premise of crushing, the energy absorbed by the middle layer due to shape change is greater than that of the lower layer and upper layer. From the perspective of energy conversion, the coal samples under the path in the middle layer have many developed cracks and the largest damage degree, followed by that in the lower layer and the upper layer. This finding is consistent with the experimental results of the true triaxial test under different layers and different stress paths.

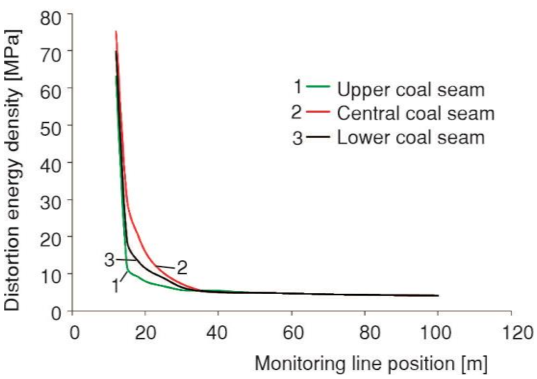

Figure 11. Variation of distortion energy density in different horizons with the position of survey line

Re-crushing of top coal above support

After the shearer finishes cutting coal, the hydraulic support is pulled, moved and lifted to couple the hydraulic support with the top coal. During this period, due to the power provided by the hydraulic pump station, the oil cylinder is extended, and the support pillar is lifted to act on the top coal to implement active restraint and generate additional stress. At this time, the stress state of the top coal is changed from two-dimensional stress to 3-D stress. To prevent discontinuous deformation and damage (such as delamination of the top coal), the support pillar has a certain initial support force [13], which is generally 70-80% of the rated working resistance of the support. In the Tashan mining area, the initial support force of the caving support is not less than 12000 kN. At this time, the support of the support restricts the longitudinal displacement of the top coal. After the top coal is discharged, the support moves forward in the advancing direction, and the stress on the top coal is changed from 3-D force to the 2-D force. The support moves forward and the coal discharging step is generally not long (about 1 m), and the control top is about 5m from the top coal. Therefore, the support repeatedly supports the lower layer of the top coal 4 or 5 times. The repeated unloading and support of the support directly damage the top coal above the support. To a certain extent, it also determines the periodic changes of the internal stress of the top coal at the micro level and the subsidence of the top coal at the macro level. As a result, the top coal is in an alternating and repetitive stress field, which affects the crushing of the top coal. Therefore, the repeated support of the hydraulic support can loosen the top coal and promote the crushing of the top coal to a certain extent.

Failure structure model of top coal in extra-thick coal seam

Under the influence of mining activities, overburden movement and support, the spatial stress of the stope is redistributed, and the stress evolution of different positions from the coal wall and different layers of the top coal is different, resulting in the difference of distortion energy density. In this study, the failure structure model of top coal is proposed, as shown in fig 12. In this model, there are four stages in the horizontal direction: original rock stage, crack development stage, crushing stage, and re-crushing stage. In the original rock stage, the cracks in the top coal body have a similar development, and the coal body in this area is not affected by mining, but only by the natural fracture structural plane in the coal body. In the crack development stage, the crack development of different layers of the top coal in this area is similar, and more cracks are developed in the coal body than in the original rock stage. The stress of different layers in this stage is increased with a similar changing trend, and the distortion energy density is similar. The stress value does not reach the limit value, and the coal body fails to yield and break. In the crushing stage, the top coal has the largest crushing in the middle layer, followed by that in the lower layer, and the top coal has the smallest crushing in the upper layer. The main control factors are the front abutment pressure and the difference in the horizontal stress state in the same vertical

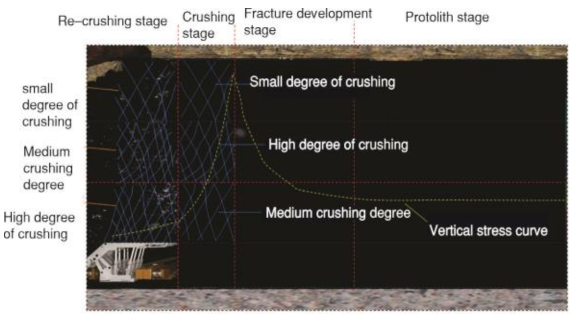

Figure 12. Failure structure model of extra thick top coal

direction. In the re-crushing stage, the lower and middle layers of the top coal in the roof control area above the support are relatively crushed, and the lumpiness of the upper layer is the largest. This is not only affected by the front abutment pressure, but also repeatedly supported by the hydraulic support.

Conclusion

By using FLAC numerical simulation, the evolution law of principal stress in different layers of top coal in the extra-thick coal seams was studied. The position of peak principal stress is about 12 m in front of the coal wall. Within the range of 0-25 m in front of the coal wall, three principal stresses in the same vertical direction of different top coal layers are different. According to the stress evolution characteristics of different layers of extra-thick coal seams, the true triaxial loading test on coal rock was carried out. The research results show that the samples experienced the compaction stage, linear elastic stage and plastic failure stage, and the stress state of the samples at failure is consistent with that obtained by numerical simulation. And it indicates that there is the largest cracks in the middle layer of the coal sample, a moderate cracks in the lower layer of the coal sample, and the weakest cracks in the upper layer of the coal sample. This phenomenon is also explained by the distortion energy density theory. Based on the stress evolution law in different layers of extra-thick coal seams and true triaxial experiments, the failure structure model of top coal was constructed. In this model, there are four stages in the horizontal direction: original rock stage, crack development stage, crushing stage and re-crushing stage, and the broken blocks of top coal in different layers in the vertical direction show multiple levels.

Acknowledgment

This study was financially supported by National Key R&D Program of China (Grant No. 2018YFC0604502), and Natural Science Foundation of Henan Province (Grant No. 202300410175).

References

[1] Wang, J. C., *et al.*, Engineering Practice and Theoretical Progress of Top-coal Caving Mining Technology in China, *Journal of China Coal Society*, *43* (2018), 1, pp. 43-51
[2] Si, Q. B., *et al.*, Energy Supplyplanning of the Five Northwest Province in 2030 Under Carbon Intensity and Water Resource Constraints, *Journal of XI'An Jiaotong University*, *56* (2022), 5, pp. 31-42
[3] Xu, S. S., *et al.*, Coal Scientific Production Capacity and Resource Guarantee Level Analyses in China, *Coal geology of China*, *23* (2011), 8, pp. 1-8
[4] Wang, J. C., *et al.*, The Present Status and the Key Issues to Be Resolved of Thick Seam Mining Technique in China, *Sciencepaper Online*, (2008), 11, pp. 829-834
[5] Hu, S. R., *et al.*, Distribution and Genetic Model of Extra-thick Coal Seams, *Coal Geology of China*, *23* (2011), 1, pp. 1-5
[6] Song, X. M., *et al.*, Advances on Longwall Fully-mechanized Top-coal Caving Miningtechnology in China During Past 40 years: theory, equipment and approach, *Coal Science and Technology*, *49* (2021), 3, pp. 1-29
[7] Wang, J. H., *et al.*, Layout Strategic Research of Green Coal Resource Development in China, *Journal of China University of Ming&Technology*, *47*. (2018) , 1, pp. 15-20
[8] Vakili A., *et al.*, A New Cavability Assessment Criterion for Longwall Top Coal Caving, *International Journal of Rock Mechanics and Mining Sciences*, *47*. (2010) , 8, pp. 1317-1329
[9] Kang, X., *et al.*, Analysis on Top Coal Broken Mechanism of Fully-mechanized Coal Caving Faces, *Coal Engineering*, *49*. (2017) , 8, pp. 107-109
[10] Huo, Y. M., Research on Failure Mechanism and Intelligent Drawing Control of Top Coal in Thick Coal Seam, Ph. D. thesis, Taiyuan University of Technology, Taiyuan, China, 2021

[11] Alehossein H., *et al.*, Stress Analysis of Longwall Top Coal Caving, *International Journal of Rock Mechanics and Mining Sciences*, *47*. (2010), 1, pp. 30-41
[12] Yang, X. J., *et al.*, On the Theory of the Fractal Scaling-law Elasticity, *Meccanica*, *57* (2022), 4, pp.943-955
[13] He, Y. S., Study on AE Testing Method of Microscopic Mechanism of Rock Failure Based on Moment Tensor, Ph. D. thesis, Chengdu University of Technology, Chengdu, China, 2017

Paper submitted: August 15, 2022
Paper revised: December 5, 2022
Paper accepted: December 18, 2022